Molecular Pharmacology Fast Forward. Published on November 8, 2019 as DOI: 10.1124/mol.119.118091
This article has not been copyedited and formatted. The final version may differ from this version.

MOL # 118091

Title Evaluation of operational models of agonism and allosterism at receptors with multiple orthosteric binding sites

Authors Karen J. Gregory[1], Jesús Giraldo[2,3,4], Jiayin Diao[1], Arthur Christopoulos[1] and Katie Leach[1]

Affiliations [1]Drug Discovery Biology and Department of Pharmacology, Monash Institute of Pharmaceutical Sciences, Monash University, Parkville, Australia; [2]Laboratory of Molecular Neuropharmacology and Bioinformatics, Institut de Neurociències and Unitat de Bioestadística, Facultat de Medicina, Universitat Autònoma de Barcelona, Spain; [3]Instituto de Salud Carlos III, Centro de Investigación Biomédica en Red de Salud Mental, CIBERSAM, 08193, Bellaterra, Spain; [4]Unitat de Neurociència Traslacional, Parc Taulí Hospital Universitari, Institut d'Investigació i Innovació Parc Taulí (I3PT), Institut de Neurociències, Universitat Autònoma de Barcelona, 08193 Bellaterra, Spain

Molecular Pharmacology Fast Forward. Published on November 8, 2019 as DOI: 10.1124/mol.119.118091
This article has not been copyedited and formatted. The final version may differ from this version.

MOL # 118091

Running title Operational models for receptors with multiple agonist sites

Corresponding author

Katie Leach

Drug Discovery Biology and Department of Pharmacology, Monash Institute of Pharmaceutical Sciences, Monash University, 399 Royal Parade, Parkville, Australia

+61 3 9903 9089

katie.leach@monash.edu

Number of text pages 28

Number of tables 6

Number of figures 7

Number of references 33

Number of words in the abstract 232

Number of words in the introduction 666

Number of words in the discussion 912

Abbreviations CaSR, calcium-sensing receptor; PAM, positive allosteric modulator; mAChR, muscarinic acetylcholine receptor; mGlu, metabotropic glutamate receptor; NAM, negative allosteric modulator; pERK1/2, extracellular regulated kinase 1/2 phosphorylation

Molecular Pharmacology Fast Forward. Published on November 8, 2019 as DOI: 10.1124/mol.119.118091
This article has not been copyedited and formatted. The final version may differ from this version.

Abstract

Current operational models of agonism and allosterism quantify ligand actions at receptors where agonist concentration-response relationships are non-hyperbolic by introduction of a transducer slope that relates receptor occupancy to response. However, for some receptors, non-hyperbolic concentration-response relationships arise from multiple endogenous agonist molecules binding to a receptor in a cooperative manner. Thus, we developed operational models of agonism in systems with cooperative agonist binding, and evaluated the models by simulating data describing agonist effects. The models were validated by analyzing experimental data demonstrating the effects of agonists and allosteric modulators at receptors where agonist binding follows hyperbolic (M_4 muscarinic acetylcholine receptors) or non-hyperbolic relationships (metabotropic glutamate receptor 5 and calcium-sensing receptor). For hyperbolic agonist-concentration response relationships, no difference in estimates of ligand affinity, efficacy or cooperativity were observed when the slope was assigned to either a transducer slope or to an agonist binding slope. In contrast, for receptors with non-hyperbolic agonist concentration-response relationships, estimates of ligand affinity, efficacy or cooperativity varied depending on the assignment of the slope. The extent of this variation depended upon the magnitude of the slope value, agonist efficacy, and, for allosteric modulators, on the magnitude of cooperativity. The modified operational models described herein are well suited to analyzing agonist and modulator interactions at receptors that bind multiple orthosteric agonists in a cooperative manner. Accounting for cooperative agonist binding is essential to accurately quantify agonist and drug actions.

Significance statement

Some orthosteric agonists bind to multiple sites on a receptor, but current analytical methods to characterize such interactions are limited. Herein, we develop and validate operational

models of agonism and allosterism for receptors with multiple orthosteric binding sites, and demonstrate that such models are essential to accurately quantify agonist and drug actions. These findings have important implications for the discovery and development of drugs targeting receptors such as the calcium-sensing receptor, which binds at least five calcium ions.

Introduction

The past 30 years have seen major advances in quantifying the relationship between receptor occupancy and response, with the operational model of agonism (Black and Leff, 1983) representing one of the most common analytical approaches. The operational model of agonism describes agonist effects based on agonist affinity (K_A) and observed efficacy in a given test system. The latter is defined by a transducer ratio, τ, which is a function of both tissue- and agonist-specific components; it is the ratio of the total receptor number (R_T) and a transducer parameter (K_E) that defines the avidity with which a given agonist-occupied receptor complex promotes the final observed pharmacological effect. As such, the operational model of agonism is a useful tool for quantifying agonism in a comparable manner across different test systems (Black and Leff, 1983), and has subsequently been extended or modified to also quantify effects of allosteric modulators and biased agonists (Kenakin, 2012; Leach et al., 2010; Leach et al., 2007).

The operational model of agonism has been most commonly applied to characterize the activity of agonists that display both rectangular hyperbolic or non-hyperbolic concentration-response curves, i.e., normally empirically characterized by Hill slopes that are equal to or different from unity, respectively. The key underlying assumption in the majority of instances to date where an agonist concentration-response curve displays a Hill slope significantly

Molecular Pharmacology Fast Forward. Published on November 8, 2019 as DOI: 10.1124/mol.119.118091
This article has not been copyedited and formatted. The final version may differ from this version.

different from 1 has been ascribed in the most common form of the operational model to differences in the post-receptor machinery that transduce occupancy to response, i.e., through introduction of a so-called "transducer slope" (*n*) (Black et al., 1985). For instance, steep or shallow Hill slopes could arise due to changes in the sensitivity of one or more steps in a receptor's signal transduction mechanism, while the initial agonist-receptor binding event is assumed to be characterized by a simple hyperbolic one-to-one relationship. However, for ion channels and a number of G protein-coupled receptors (GPCRs), particularly the class C GPCR subfamily, non-hyperbolic concentration-response relationships can also arise from cooperative binding of multiple equivalents of the same endogenous agonist molecule prior to any subsequent processing of the stimulus by the cellular transduction machinery. For example, while a number of small molecule calcium-sensing receptor (CaSR) agonists produce responses characterized by Hill slopes close to unity (Cook et al., 2015; Keller et al., 2018), indicating a transducer slope equal to unity, it is also well established that CaSR responses to its endogenous activator, extracellular calcium (Ca^{2+}_o) and other divalent cations are characterized by extremely high Hill slopes, ranging from 2 to 4 (Brown, 1983; Davey et al., 2012; Leach et al., 2015). The most parsimonious explanation to account for these disparate observations is that the operational transducer slope linking CaSR agonist occupancy to response can adequately be described by a transducer slope equal to unity, which suggests that the cooperativity observed in response to activators such as (Ca^{2+}_o) ions arises at the level of binding, not function. This is also in accord with known pharmacological and structural studies of the CaSR that have identified multiple binding sites for Ca^{2+}_o ions (Geng et al., 2016). As a consequence, the classic operational model of agonism as applied to concentration-response curves of non-unit Hill slopes is suboptimal for such situations.

Molecular Pharmacology Fast Forward. Published on November 8, 2019 as DOI: 10.1124/mol.119.118091
This article has not been copyedited and formatted. The final version may differ from this version.

Herein, we sought to develop and evaluate an operational model of agonism that describes orthosteric agonist binding to multiple sites in a cooperative manner, referred to as the "cooperative agonist operational model". The cooperative agonist operational model was superior to the original Black and Leff operational model of agonism in fitting Ca^{2+}_o-CaSR concentration-response data. We also extended this cooperative agonist operational model to incorporate allosteric modulation of the affinity and efficacy of an agonist that binds cooperatively to multiple sites. This "operational model of allosterism with cooperative agonist binding" was fitted to data describing the actions of CaSR positive allosteric modulators (PAMs) and negative allosteric modulators (NAMs), and revealed that if cooperative agonist binding is not taken into consideration, under- or overestimates of PAM and NAM affinity and cooperativity can occur.

Materials and methods

Materials

Dulbecco's modified Eagle's medium (DMEM), FlpIn HEK TREx cells, blasticidin S HCl and FBS were obtained from Invitrogen (Carlsbad, USA), whilst hygromycin B was from Roche (Mannheim, Germany). Fluo-8 AM was from Abcam (Cambridge, MA, USA).

CaSR-expressing HEK293 cell lines

The generation of DNA and FlpIn HEK TREx cells stably expressing c-myc-tagged WT CaSR in pcDNA5/frt/TO have been described previously (Davey et al., 2012; Leach et al., 2016). FlpIn HEK TREx CaSR cells were maintained in DMEM containing 5% FBS, 200 μg/mL hygromycin B and 5 μg/mL blasticidin S HCl. To generate a tetracycline-inducible FlpIn HEK cell line stably expressing an N terminally-truncated CaSR, N terminally-truncated CaSR corresponding to amino acids 600-903 with an N-terminal influenza

Molecular Pharmacology Fast Forward. Published on November 8, 2019 as DOI: 10.1124/mol.119.118091
This article has not been copyedited and formatted. The final version may differ from this version.

haemagglutinin signal peptide followed by a c-myc epitope and rhodopsin signal peptide in pcDNA3.1+ (Leach et al., 2016) was transferred to pcDNA5/frt/TO using BamHI and NotI restriction sites. FlpIn HEK TREx cells were seeded into 25 cm^2 flasks in DMEM containing 5% FBS and allowed to reach 80% confluency. Cells were transfected with 0.5 μg pcDNA5/frt/TO containing the N terminally-truncated CaSR plus 5 μg POG44 with lipofectamine 2000 (1:4 DNA:lipofectamine 2000) according to manufacturer's instructions. The following day, cells were transferred to a T75 cm^2 flask, and 24 hrs later DMEM was replaced with DMEM containing 5% FBS, 200 μg/mL hygromycin and 5 μg/mL blasticidin S HCl. Selection DMEM was replaced every 3 days until untransfected cells had died (~10 days), and antibiotic-resistant cells were expanded and maintained in DMEM containing 5% FBS, 200 μg/mL hygromycin and 5 μg/mL blasticidin S HCl. All cell lines were routinely tested for mycoplasma contamination using the Lonza™ MycoAlert™ mycoplasma detection kit.

Determination of WT and N terminally-truncated CaSR cell surface expression using FACs

FlpIn HEK TREx WT and N terminally-truncated CaSR expressing cells were seeded at 80,000 cells/well into a 96-well plate and expression was induced with 100 ng/mL tetracycline overnight at 37^{o}C. The following day, cells were harvested, washed in 1 x PBS with 0.1% BSA and 2 mM EDTA (wash buffer) by centrifugation (350 x g, 4^{o}C for 3 min) before resuspension and 30 min incubation in 100 μL blocking buffer (1 x PBS, 5% BSA and 2 mM EDTA) containing 1 μg/mL AF647-conjugated 9E10 made in house as previously described (Cook et al., 2015). Cells were washed as previously described and resuspended in wash buffer containing propidium iodide. Live cell fluorescence was measured using a FACS Canto (Becton Dickinson).

Molecular Pharmacology Fast Forward. Published on November 8, 2019 as DOI: 10.1124/mol.119.118091
This article has not been copyedited and formatted. The final version may differ from this version.

Calcium mobilization assays

Cells were seeded in clear 96-well plates coated with poly-D-lysine (50 μg mL^{-1}) at 80,000 cells/well and incubated overnight in the presence of 0 or 100 ng mL^{-1} tetracycline. The following day, cells were washed with assay buffer (150 mM NaCl, 2.6 mM KCl, 1.18 mM $MgCl_2$, 10 mM D-Glucose, 10 mM HEPES, 0.1 mM $CaCl_2$, 0.5 % BSA and 4 mM probenecid at pH 7.4) and loaded with Fluo-8 AM (1 μM in assay buffer) for 1 h at 37 ^oC. Cells were washed with assay buffer prior to the addition of fresh assay buffer.

For all studies, each well was treated with a single agonist concentration. The release of Ca^{2+}_i was measured at 37°C using a Flexstation® 1 or 3 (Molecular Devices; Sunnyvale, California). Fluorescence was detected for 60 sec at 490 nm excitation and 520 nm emission and the peak Ca^{2+}_i mobilization response (approximately 12 sec after agonist addition) was used for the subsequent determination of the agonist response. Relative peak fluorescence units were normalized to the fluorescence stimulated by 1 μM ionomycin to account for differences in cell number and loading efficiency.

Model derivation and data analysis

The derivation of operational models describing the effect of an agonist in the absence or presence of an allosteric modulator at a receptor with multiple agonist binding sites is presented in Appendix 1. The script input to use the two equations in the program, Graphpad Prism, is also presented in the Appendix.

Data simulations were performed using the original Black and Leff operational model of agonism, referred to herein as the Black and Leff model (Eq 1), or a modified cooperative agonist operational model (Eq 2), where an additional slope (*nB*) was incorporated to account

Molecular Pharmacology Fast Forward. Published on November 8, 2019 as DOI: 10.1124/mol.119.118091
This article has not been copyedited and formatted. The final version may differ from this version.

for multiple agonist binding sites and thus the steepness of the slope describing the agonist concentration–occupancy relationship.

$$\text{Effect}=\frac{E_m{\tau_A}^{nT}[A]^{nT}}{{\tau_A}^{nT}[A]^{nT}+([A]+K_A)^{nT}}$$

Eq 1

$$\text{Effect}=\frac{E_m{\tau_A}^{nT}[A]^{nBnT}}{{\tau_A}^{nT}[A]^{nBnT}+\left([A]^{nB}+{K_A}^{nB}\right)^{nT}}$$

Eq 2

where [A] is the agonist concentration, K_A is the agonist equilibrium dissociation constant; τ_A is an operational measure of agonist efficacy; E_m is the maximal system response; *nT* is the transducer slope linking agonist concentration to response; and *nB* is the binding slope linking agonist concentration to receptor occupancy.

For simplicity, the modified cooperative operational model of agonism (Eq 2) makes the following assumptions:

i. The receptor is either empty or fully occupied, and only the fully occupied receptor exerts an effect. The lack of partially occupied receptor molecules could arise if multiple agonist molecules bind simultaneously to the receptor, or if agonist molecules bind sequentially with high positive cooperativity. Thus, once one binding site is occupied, positive cooperativity drives occupancy of all other sites. The latter scenario is most likely, hence why we have called this model the cooperative agonist operational model.

ii. The model cannot discern cooperativity between the multiple binding sites, thus *nB* may not be the true number of binding sites. *nB* is therefore a binding slope coefficient;

Molecular Pharmacology Fast Forward. Published on November 8, 2019 as DOI: 10.1124/mol.119.118091
This article has not been copyedited and formatted. The final version may differ from this version.

iii. K_A is a geometric mean of the microscopic dissociation constants for each binding site.

Agonist concentration response curves were fitted to Eq 1 or 2 to quantify agonist affinity and efficacy. When fitting experimental data to Eq 2, the transducer slope was constrained to unity (see Results for validation of this assumption).

Data describing the interaction between glutamate and PAMs and NAMs at $mGlu_5$, or between ACh and LY2033298 at the M_4 muscarinic acetylcholine receptor (mAChR), were fitted to our original operational model of allosterism (Eq 3) or to the new operational model of allosterism with cooperative agonist binding (Eq 4). For simplicity and for the purpose of fitting experimental data, Eqs 3-8 assume a single allosteric modulator binding site, and therefore do not account for modulator cooperative binding.

$$\text{Effect}=\frac{E_m(\tau_A[A](K_B+\alpha\beta[B])+\tau_B[B][K_A])^{nT}}{([A]K_B+K_AK_B+K_A[B]+\alpha[A][B])^{nT}+(\tau_A[A](K_B+\alpha\beta[B])+\tau_B[B]K_A)^{nT}}$$

Eq 3

$$\text{Effect}=\frac{E_m\left(\tau_A[A]^{nB}(K_B+\alpha\beta[B])+\tau_B[B][K_A]^{nB}\right)^{nT}}{\left([A]^{nB}K_B+{K_A}^{nB}K_B+{K_A}^{nB}[B]+\alpha[A]^{nB}[B]\right)^{nT}+\left(\tau_A[A]^{nB}(K_B+\alpha\beta[B])+\tau_B[B]{K_A}^{nB}\right)^{nT}}$$

Eq 4

where K_A is the equilibrium dissociation constant of the orthosteric agonist and was fixed in some instances to the affinity determined in radioligand binding assays (Leach et al., 2010; Mutel et al., 2000); K_B is the equilibrium dissociation constant of the allosteric ligand; τ_A and τ_B are the operational efficacies of the orthosteric agonist and allosteric ligand, respectively; α and β are the allosteric effects on orthosteric agonist affinity and efficacy, respectively (it should be noted that β is not a reciprocal efficacy cooperativity factor (Giraldo, 2015; Leach et al., 2007)); [A] and [B] are the orthosteric agonist and allosteric ligand concentrations,

Molecular Pharmacology Fast Forward. Published on November 8, 2019 as DOI: 10.1124/mol.119.118091
This article has not been copyedited and formatted. The final version may differ from this version.

respectively; E_m is the maximal system response; *nT* is the transducer slope linking agonist concentration to response; and *nB* is the slope of agonist binding linking agonist concentration to occupancy.

To fit the operational model of allosterism to data describing the interaction between Ca^{2+}_o and cinacalcet at the CaSR, the original operational model of allosterism shown by equation 3 was simplified, because for a full agonist like Ca^{2+}_o (i.e., one that generates the maximal system response at submaximal receptor occupancies), K_A >> [A]. Further, because the CaSR's orthosteric agonist, Ca^{2+}_o, was present in the assay buffer, contaminating agonist was included in the equations used to analyze CaSR PAM (cinacalcet) and NAM (NPS2143) data (Keller et al., 2018). Therefore, data describing the interaction between Ca^{2+}_o and cinacalcet or NPS2143 at the CaSR were fitted to the original operational model of allosterism with contaminating agonist (Eqs 5 and 6, respectively) or to an operational model of allosterism with cooperative agonist binding and contaminating agonist (Eqs 7 and 8, respectively):

$$\text{Effect}=\frac{E_m([A+C](K_B+\alpha\beta[B])+\tau_B[B][EC_{50}])^{nT}}{[EC_{50}]^{nT}(K_B+[B])^{nT}+([A+C](K_B+\alpha\beta[B])+\tau_B[B][EC_{50}])^{nT}}$$

Eq 5

where EC_{50} is the agonist concentration that elicits a half maximal response (it should be noted that inclusion of [EC_{50}] involves some simplifying assumptions that facilitate data fitting (Aurelio et al., 2009; Giraldo, 2015)); [C] is the contaminating agonist concentration; and all other parameters are as described for Eq 3.

$$\text{Effect}=\frac{E_m(\tau_A[A+C](K_B+\alpha\beta[B])+\tau_B[B][K_A])^{nT}}{([A]K_B+K_AK_B+K_A[B]+\alpha[A+C][B])^{nT}+(\tau_A[A+C](K_B+\alpha\beta[B])+\tau_B[B]K_A)^{nT}}$$

Eq 6

where [C] is the contaminating agonist concentration and all other parameters are as described for Eq 3.

Molecular Pharmacology Fast Forward. Published on November 8, 2019 as DOI: 10.1124/mol.119.118091
This article has not been copyedited and formatted. The final version may differ from this version.

$$\text{Effect}=\frac{E_m\left([A+C]^{nB}(K_B+\alpha\beta[B])+\tau_B[B][EC_{50}]^{nB}\right)^{nT}}{[EC_{50}]^{nBnT}(K_B+[B])^{nT}+\left([A+C]^{nB}(K_B+\alpha\beta[B])+\tau_B[B][EC_{50}]^{nB}\right)^{nT}}$$

Eq 7

where EC_{50}, K_B, τ_B, α, β, [A], [B], [C] and E_m are as described for Eq 5 and *nB* is the slope of agonist binding linking agonist concentration to occupancy.

$$\text{Effect}=\frac{E_m\left(\tau_A[A+C]^{nB}(K_B+\alpha\beta[B])+\tau_B[B][K_A]^{nB}\right)^{nT}}{\left([A+C]^{nB}K_B+K_A{}^{nB}K_B+K_A{}^{nB}[B]+\alpha[A+C]^{nB}[B]\right)^{nT}+\left(\tau_A[A]^{nB}(K_B+\alpha\beta[B])+\tau_B[B]K_A{}^{nB}\right)^{nT}}$$

Eq 8

where [C] is the contaminating agonist concentration and all other parameters are as described for Eq 4.

Simulated data was fitted to the following Hill equation:

$$\text{Effect}=\frac{[A]^{nH}E_{max}}{[A]^{nH}+EC_{50}{}^{nH}}$$

Eq 9

where [A] is agonist concentration; E_{max} is the maximum agonist effect; EC_{50} is the agonist concentration that produces half the maximum agonist effect; and *nH* is the Hill slope.

Non-linear regression analysis was performed in GraphPad Prism 7 or 8. Potency, affinity, cooperativity and efficacy parameters were estimated as logarithms (Christopoulos, 1998). An extra sum of squares F test was used to determine whether data were fitted best when the Hill slope, binding slope or transducer slope (*nH*, *nB* or *nT*, respectively) were significantly different from unity, where $p < 0.05$ was considered significant.

Molecular Pharmacology Fast Forward. Published on November 8, 2019 as DOI: 10.1124/mol.119.118091
This article has not been copyedited and formatted. The final version may differ from this version.

Results

The contribution of slope factors to agonist concentration-response relationships

We first evaluated the contribution of the agonist binding slope (*nB*) or transducer slope (*nT*) to the concentration-response curve of two agonists with different efficacies, by simulating variations in *nB* or *nT* using the cooperative agonist operational model (Eq 2). We specifically wanted to evaluate a system with cooperative agonist binding, therefore we based our simulations on Ca^{2+}_o activation of the CaSR. The Ca^{2+}_o concentration-response relationship for the CaSR's best characterized physiological role, inhibition of parathyroid hormone (PTH) secretion, occurs over a Ca^{2+}_o concentration range of 0.8 – 1.5 mM with an EC_{50} of ~1.2 mM (Brown, 1983). Thus, for these simulations, the affinity of the agonist (K_A) was assumed to be 1.2 mM and *nB* or *nT* were assumed to be between 1 and 3. Simulated data was subsequently fitted to a Hill equation (Eq 9). Unsurprisingly, increasing *nB* or *nT* increases the Hill slope of the agonist concentration-response curve (Figure 1, Table 1). Further, increasing *nT* decreases agonist potency. Interestingly, the effect of *nB* on agonist potency depends on the magnitude of *nT* and τ_A. For instance, increasing *nB* decreases agonist potency for higher efficacy agonists (τ_A 3). However, for lower efficacy agonists (τ_A 1), increasing *nB* decreases agonist potency when *nT* is ≤1, but increases agonist potency when *nT* is ≥2.

We next sought to directly compare the influence of the binding or transducer slope by simulating concentration-response curves for agonists with varying efficacies using the Black and Leff operational model (Eq 1, which contains a transducer slope, *nT*) and the cooperative agonist operational model (Eq 2, which contains a transducer and a binding slope, *nT* and *nB*, respectively). As can be seen in Figure 2 and Table 2, when *nT* or *nB* are equal to 1, variations in τ_A have an identical effect on empirical agonist concentration-response

Molecular Pharmacology Fast Forward. Published on November 8, 2019 as DOI: 10.1124/mol.119.118091
This article has not been copyedited and formatted. The final version may differ from this version.

parameters (potency, Hill slope or E_{max}) regardless of the model. In contrast, when *nT* or *nB* are greater than 1, variations in τ_A result in major differences in the agonist concentration-response profile predicted with the two different operational models of agonism. Specifically, the Black and Leff model predicts that high efficacy agonists have greater potency relative to affinity (due to amplification of the "steps" between agonist binding and response), while for low efficacy agonists, the EC_{50} may be less than the K_A for curves that possess non-unity Hill slopes. The latter was previously noted by Black and Leff (Black et al., 1985). Further, the Hill slope decreases alongside decreases in τ_A. In comparison, the cooperative agonist operational model predicts that when *nT* is 1, agonist EC_{50} may approach but not be less than its K_A, regardless of whether *nB* is greater than 1, and there is no effect of τ_A on the Hill slope of the agonist concentration-response curve (Figure 2, Table 2).

Quantification of experimentally derived agonist concentration-response data

We next tested whether our simulations were recapitulated in a functional assay that measures CaSR activation. To do so, we measured Ca^{2+}_o-mediated Ca^{2+}_i mobilization following titration of CaSR expression using a tetracycline inducible system. In the absence of tetracycline, the maximal response to Ca^{2+}_o is approximately 50% of the maximal response obtained under full induction of receptor expression (100 ng/mL tetracycline). In this system, fitting a Hill equation (Eq 9) to both data sets indicated that the data were fitted best when the Hill slope was unchanged with different receptor expression levels (i.e. different magnitudes of τ_A) ($p < 0.05$, extra sum-of-squares F test; data not shown). For the CaSR, the small molecule allosteric agonists, AC265347 or calcimimetic B, activate the CaSR with a Hill slope of 1 (Cook et al., 2015; Keller et al., 2018). Similarly, when cooperative agonist binding is prevented by removal of the CaSR's N terminal domain and consequently the primary Ca^{2+}_o binding sites, the Hill slope for Ca^{2+}_o is not significantly different to unity (see

Molecular Pharmacology Fast Forward. Published on November 8, 2019 as DOI: 10.1124/mol.119.118091
This article has not been copyedited and formatted. The final version may differ from this version.

below). This provides experimental evidence that the CaSR's transducer slope is equal to unity, and that the steep Hill slopes observed for Ca^{2+}_o at the full-length CaSR thus likely arise from a binding slope greater than 1. Thus, when fitting CaSR experimental data to the cooperative agonist operational model, *nT* was constrained to unity.

When the data were fitted to the classic Black and Leff model, the estimated K_A was 0.2 mM (Figure 3A, Table 3). In comparison, the cooperative agonist operational model yielded a K_A estimate of 1.1mM, which is in close agreement with the EC_{50} (1.2 mM) of Ca^{2+}_o for suppressing PTH release (Brown, 1983) and Ca^{2+}_o affinity estimates for the CaSR extracellular domain determined using spectroscopic approaches (Huang et al., 2009; Zhang et al., 2014). For both analyses, data were fitted best when the binding slope (cooperative agonist operational model) or transducer slope (Black and Leff model) were different to unity ($p < 0.05$, extra sum of squares F test).

To further validate our simulations in a functional assay, we next sought to quantify the affinity and efficacy of a CaSR partial agonist. To do so, we took advantage of observations that in comparison to at the WT CaSR (Figure 3B), Ca^{2+}_o acting via the 7 transmembrane (7TM) domain is a partial agonist at an N-terminally truncated CaSR (depicted in Figure 3C) relative to the trivalent cation, gadolinium (Gd^{3+}_o) (Figure 3D). FACs analysis confirmed cell surface expression of the WT and N terminally-truncated CaSR (Supplemental Figure 1). We quantified Ca^{2+}_o affinity and efficacy at the N terminally-truncated CaSR using the original Black and Leff model or the cooperative agonist operational model (Table 3). In both instances, data were best fitted when the binding slope (cooperative agonist operational model) or transducer slope (Black and Leff model) were not different to unity ($p < 0.05$, extra sum of squares F test), consistent with a reduction in positively cooperative Ca^{2+}_o binding, as

Molecular Pharmacology Fast Forward. Published on November 8, 2019 as DOI: 10.1124/mol.119.118091
This article has not been copyedited and formatted. The final version may differ from this version.

would be expected upon removal of the four primary Ca^{2+}_o binding sites located in the N terminal domain (Geng et al., 2016). Thus, parameters determined at the N terminally-truncated receptor were identical regardless of the equation used to analyze the data. Ca^{2+}_o affinity and cooperativity estimates at the N terminally-truncated receptor were compared to those determined at the full-length WT CaSR, indicating a reduction in Ca^{2+}_o affinity at the N terminally-truncated receptor in comparison to WT (Table 3), again consistent with removal of the primary Ca^{2+}_o binding sites. However, due to a lower estimate of Ca^{2+}_o efficacy at the WT receptor when WT data were analyzed using the Black and Leff model, only the cooperative agonist operational model accurately quantified a reduction in Ca^{2+}_o efficacy at the N terminally-truncated receptor in comparison to at the WT receptor. This is consistent with a lower Ca^{2+}_o E_{max} at the N terminally-truncated receptor (~60% of the maximum response stimulated by Gd^{3+}_o) in comparison to WT (~100% Gd^{3+}_o E_{max}) (Table 3). Thus, only the cooperative agonist operational model accurately estimated Ca^{2+}_o partial agonism at the N terminally-truncated receptor.

Quantifying allosteric interactions in systems with different degrees of cooperative agonist binding

Having established that the cooperative agonist operational model best fitted our Ca^{2+}_o-WT CaSR concentration-response curves with Hill slopes greater than 1, we next extended this model to allow for quantification of allosteric modulation of an agonist response. The operational model of agonism and allosterism (Leach et al., 2010; Leach et al., 2007) (referred to herein as the original operational model of agonism and allosterism) combines the allosteric ternary complex models developed by Stockton et al. and Ehlert (Ehlert, 1988; Stockton et al., 1983) and the Black and Leff operational model of agonism, to account for allosteric effects on agonist affinity and efficacy. In our original model (Leach et al., 2007),

the allosteric modulator can also possess intrinsic efficacy. Introduction of a slope in that model once again assumed that the slope linked occupancy to response, not to the original binding events, which were assumed to be described as simple one-to-one hyperbolic functions. Therefore, we adapted this operational model of allosterism to account for cooperative agonist binding, referred to hereafter as the "operational model of allosterism with cooperative agonist binding". In order to validate this operational model of allosterism with cooperative agonist binding, we reanalyzed existing data demonstrating positive and negative allosteric modulation at three model GPCRs with different agonist Hill slopes: CaSR (a class C GPCR where the primary endogenous agonist, Ca^{2+}_o, has a Hill slope of 2 – 4), $mGlu_5$ (a class C GPCR where the primary endogenous agonist, L-glutamate, has a Hill slope of ~1.8) (Sengmany and Gregory, 2016), and M_4 mAChR (a class A GPCR where the endogenous agonist, acetylcholine, has a Hill slope of 1) (Leach et al., 2011; Leach et al., 2010) (Supplemental Figure 2). In all instances, *nT* was assumed to be unity and all allosteric modulators were assumed to bind to a single site (i.e. the modulator binding slope is unity).

For the CaSR, we analyzed allosteric modulation of Ca^{2+}_o by cinacalcet (PAM) or NPS2143 (NAM) (Leach et al., 2016) with the original operational model of agonism and allosterism with contaminating (i.e., ambient buffer) agonist (Eq 5 or 6, respectively) and the newly derived operational model of allosterism with cooperative agonist binding and contaminating agonist (Eq 7 or 8, respectively) (Figure 4). Similar to our analysis of agonist concentration-response curves, data were fitted best when the binding slope (operational model of allosterism with cooperative agonist binding) or transducer slope (original operational model of agonism and allosterism) were different to unity ($p < 0.05$, extra sum of squares F test). Compared to the original operational model of agonism and allosterism, the estimated affinity for Ca^{2+}_o determined using the operational model of allosterism with cooperative agonist

Molecular Pharmacology Fast Forward. Published on November 8, 2019 as DOI: 10.1124/mol.119.118091
This article has not been copyedited and formatted. The final version may differ from this version.

binding (1.4 mM; Table 4) was once again closer to the assumed Ca^{2+}_o affinity based on its EC_{50} for suppression of PTH release (1.2 mM) and quantification of the Ca^{2+}_o K_A at the extracellular domain using spectroscopic approaches (3-5 mM) (Huang et al., 2009; Zhang et al., 2014). Further, the estimated affinity and negative cooperativity of NPS2143 were greater (5.5- and 35-fold, respectively) when cooperative agonist binding was factored into the analysis (Table 4). For the PAM, cinacalcet, the operational model of allosterism with cooperative agonist binding yielded a 3-fold lower affinity estimate but an 8-fold greater magnitude of positive cooperativity.

We next analyzed allosteric modulation of glutamate at $mGlu_5$ (Eq 3 or 4) by a representative "full" NAM (MPEP) that completely inhibits glutamate-mediated activation of Ca^{2+}_i mobilization, a "partial" NAM (M-5MPEP) that only partially inhibits glutamate-mediated activation of Ca^{2+}_i mobilization (Sengmany et al., 2019), a pure PAM (VU-29) and a mixed PAM-agonist (DPFE) (Sengmany et al., 2017). Similar to analyses at the CaSR, all data were fitted best when the binding slope (operational model of allosterism with cooperative agonist binding) or transducer slope (original operational model of agonism and allosterism) were different to unity ($p < 0.05$, extra sum of squares F test). However, for each modulator, the affinity and cooperativity estimates were similar (within 3-fold) irrespective of the analytical model applied (Figure 5, Table 5). Therefore, although the glutamate-$mGlu_5$ concentration-response relationship has a Hill slope greater than unity, quantification of allosteric interactions at $mGlu_5$ is largely unaffected by whether the empirical slope is assumed to be determined by the transducer slope or the agonist binding slope.

For the M_4 mAChR, we analyzed previously published positive allosteric modulation of ACh by the PAM-agonist, LY2033298, in [^{35}S]GTPγS binding assays (Leach et al., 2010) (Eq 3 or

4). As expected, in the absence of cooperative ACh binding at the M_4 mAChR, data for the interaction between ACh and LY2033298 were fitted best by both operational models of agonism and allosterism when the slope was not different to unity ($p < 0.05$, extra sum of squares F test), and both equations therefore yielded identical estimates of affinity and cooperativity (Figure 6, Table 6).

We next sought to establish why quantification of PAM and NAM affinity and cooperativity were not greatly affected by the assignment of the slope at $mGlu_5$, where the glutamate Hill slope is greater than unity. To do so, we simulated the interaction between an orthosteric agonist and a NAM or PAM with the operational model of allosterism with cooperative agonist binding and analyzed the simulated data with the original operational model of agonism and allosterism. For these simulations, orthosteric agonist affinity (1 μM), τ_A (10), and modulator affinity (10 nM) were held constant, and different magnitudes of positive or negative cooperativity were examined alongside changes in the magnitude of cooperative agonist binding. Consistent with our analysis of $mGlu_5$ allosteric interaction data, when the agonist binding slope ranged from 1 to 2, the affinity of NAMs and PAMs estimated using the original operational model of agonism and allosterism fell within ~3-fold of the affinity simulated with the operational model of allosterism with cooperative agonist binding. Further, only the affinity of the full NAM (where αβ is assumed to approach zero) fell outside this 3-fold window once the agonist binding slope exceeded 2 (Figure 7A). Similarly, when analyzed with the original operational model of agonism and allosterism, αβ values (0.1 – 10) were within a 3-fold range of simulated data when *nT* ranged from 1 to 2. However, where the magnitude of cooperativity exceeded 10 for a PAM, or 0.1 for a NAM, the influence of cooperative agonist binding becomes more pronounced (Figure 7B). These simulations confirm that the assignment of *n* to a transducer or binding slope would not be

Molecular Pharmacology Fast Forward. Published on November 8, 2019 as DOI: 10.1124/mol.119.118091
This article has not been copyedited and formatted. The final version may differ from this version.

expected to greatly influence quantification of $mGlu_5$ allosteric modulation of glutamate for modulators with moderate cooperativity, consistent with our $Ca^{2+}{}_i$ mobilization data.

Discussion

In the current study, we have assessed operational models of agonism and allosterism that account for receptors whose agonists bind multiple binding sites in a cooperative manner. The modified models accurately fit experimental data at an exemplar GPCR, the CaSR, which has high sensitivity for $Ca^{2+}{}_o$ due to multiple $Ca^{2+}{}_o$ binding sites that are linked in a positively cooperative manner. We show that agonist Hill slopes that differ from unity and remain unchanged by alterations in receptor expression levels or cellular coupling efficiencies (i.e. where τ_A differs) may be indicative of cooperative agonist binding. We demonstrate that if a steep Hill slope such as that observed at the CaSR is attributed to the transducer slope rather than to the agonist binding slope, the Black and Leff operational model of agonism underestimates agonist efficacy and overestimates agonist affinity. Extension to allosteric interactions shows the importance of accounting for cooperative agonist binding, as different models fitted to the same allosteric interaction data yield divergent modulator affinity and cooperativity estimates. For instance, the original operational model of agonism and allosterism estimates lower CaSR PAM and NAM cooperativity values, and higher or lower affinity values, respectively. Data simulations support these findings and demonstrate that the impact of cooperative binding on estimates of modulator affinity and cooperativity is more pronounced as the magnitude of modulator cooperativity or cooperative agonist binding is increased. This was evidenced by our demonstration that for $mGlu_5$, where the glutamate Hill slope is ~1.8, differences in affinity and cooperativity are within the margin of experimental error (~3-fold range). Accordingly, for agonist-receptor concentration-response relationships with Hill slopes equal to unity, it

Molecular Pharmacology Fast Forward. Published on November 8, 2019 as DOI: 10.1124/mol.119.118091
This article has not been copyedited and formatted. The final version may differ from this version.

does not matter whether the slope is governed by the transducer slope or the agonist binding slope.

The operational models of agonism and allosterism with cooperative agonist binding have important practical uses for analyzing data at receptors that possess multiple agonist binding sites. This is particularly true for the CaSR, but also for ion channels and other GPCRs where agonist binding coefficients differ from unity, such as GPR39, which binds at least two Zn^{2+} ions and responds to Zn^{2+} with a Hill slope of 2 – 3 (Sato et al., 2016; Storjohann et al., 2008). Similarly, cooperative binding can occur across a GPCR dimer, which may account for the steep Hill slope at $mGlu_5$ demonstrated in the present study. For instance, the $mGlu_2$ orthosteric agonist, LY354740, stabilizes conformational rearrangements of a metabotropic glutamate receptor (mGlu) subtype 2 and 4 heterodimer ($mGlu_2$-$mGlu_4$) with a shallow hill slope (Moreno Delgado et al., 2017), which is increased to unity when LY354740 is prevented from binding to the $mGlu_2$ or $mGlu_4$ orthosteric binding site in the dimer. In contrast, glutamate E_{max} is reduced when it can bind to only one of the orthosteric sites in the heterodimer (Moreno Delgado et al., 2017). These findings indicate negative (LY354740) and positive (glutamate) cooperativity across the dimer, respectively. Negative cooperative binding has also been demonstrated at several class A GPCRs dimers, including the 5-HT_{2A}, A_3 adenosine, H_3 histamine and D_2 dopamine receptors (Brea et al., 2009; May et al., 2011; Sinkins and Wells, 1993; Vivo et al., 2006). Accurate quantification of ligand affinity, efficacy and cooperativity at such receptors using functional assays is critical, particularly where radioligand binding based methods are not available. Indeed, there are no commercially available radioligands for the CaSR, thus pharmacological characterization, and indeed drug discovery at this receptor, has generally relied upon functional measures of receptor activity to quantify drug actions. However, it must be noted that experimentally

derived pharmacological data for agonists with steep Hill slopes will likely only be fitted to the cooperative agonist operational model and the operational model of allosterism with cooperative agonist binding when one of either the binding or transducer slopes (*nB* or *nT*) is known and constrained as such. This was a key advantage of analyzing pharmacological data at the CaSR, where we showed experimentally that the transducer slope is 1.

Our findings have important implications for past and present drug discovery efforts at class C GPCRs and beyond. Establishing SAR profiles that dictate drug affinity and cooperativity is essential for predicting drug efficacy *in vivo*. However, underestimates of cooperativity at class C GPCRs with cooperative agonist binding may explain previous observations that class C GPCR allosteric modulators have limited cooperativity when compared to their class A GPCR counterparts. For example, PAMs with αβ values >100 have been reported for class A GPCRs (Abdul-Ridha et al., 2014; Leach et al., 2010), whereas for the CaSR, potentiation is at most 5-fold for many modulators (Cook et al., 2015; Diepenhorst et al., 2018; Leach et al., 2016). Thus, for GPCRs with cooperative agonist binding, larger differences between modulator cooperativities were likely previously unappreciated. This is important because allosteric modulator cooperativity can predict likely clinical efficacy or adverse effect liability. Inaccurate estimation of allosteric modulator affinity or cooperativity due to a failure to consider cooperative agonist binding likely also impacts interpretation of structure-function studies. If cooperativity values are narrowed, then more subtle effects of mutations on modulator cooperativity may have been missed.

In conclusion, we have validated a method for quantifying agonist and allosteric modulator actions at receptors that possess multiple agonist binding sites that interact in a cooperative manner. Our operational models of agonism and allosterism with cooperative agonist binding

Molecular Pharmacology Fast Forward. Published on November 8, 2019 as DOI: 10.1124/mol.119.118091
This article has not been copyedited and formatted. The final version may differ from this version.

more accurately quantify the actions of both orthosteric and allosteric drugs acting at GPCRs with cooperative agonist binding and may be used for future drug discovery efforts at these important receptors.

Authorship contributions

Participated in research design: Gregory, Christopoulos, Leach.

Conducted experiments: Diao.

Contributed new reagents or analytic tools: Giraldo, Christopoulos.

Performed data analysis: Diao, Gregory, Giraldo, Leach.

Wrote or contributed to the writing of the manuscript: Gregory, Giraldo, Christopoulos, Leach.

References

Abdul-Ridha A, Lane JR, Mistry SN, Lopez L, Sexton PM, Scammells PJ, Christopoulos A and Canals M (2014) Mechanistic insights into allosteric structure-function relationships at the M1 muscarinic acetylcholine receptor. *J Biol Chem* **289**(48): 33701-33711.

Aurelio L, Valant C, Flynn BL, Sexton PM, Christopoulos A and Scammells PJ (2009) Allosteric modulators of the adenosine A1 receptor: synthesis and pharmacological evaluation of 4-substituted 2-amino-3-benzoylthiophenes. *J Med Chem* **52**(14): 4543-4547.

Black JW and Leff P (1983) Operational models of pharmacological agonism. *Proceedings of the Royal Society of London Series B, Containing papers of a Biological character* **220**(1219): 141-162.

Black JW, Leff P, Shankley NP and Wood J (1985) An operational model of pharmacological agonism: the effect of E/[A] curve shape on agonist dissociation constant estimation. *Br J Pharmacol* **84**(2): 561-571.

Brea J, Castro M, Giraldo J, Lopez-Gimenez JF, Padin JF, Quintian F, Cadavid MI, Vilaro MT, Mengod G, Berg KA, Clarke WP, Vilardaga JP, Milligan G and Loza MI (2009) Evidence for distinct antagonist-revealed functional states of 5-hydroxytryptamine(2A) receptor homodimers. *Mol Pharmacol* **75**(6): 1380-1391.

Brown EM (1983) Four-parameter model of the sigmoidal relationship between parathyroid hormone release and extracellular calcium concentration in normal and abnormal parathyroid tissue. *J Clin Endocrinol Metab* **56**(3): 572-581.

Christopoulos A (1998) Assessing the distribution of parameters in models of ligand-receptor interaction: to log or not to log. *Trends in pharmacological sciences* **19**(9): 351-357.

Cook AE, Mistry SN, Gregory KJ, Furness SG, Sexton PM, Scammells PJ, Conigrave AD, Christopoulos A and Leach K (2015) Biased allosteric modulation at the CaSR engendered by structurally diverse calcimimetics. *Br J Pharmacol* **172**(1): 185-200.

Davey AE, Leach K, Valant C, Conigrave AD, Sexton PM and Christopoulos A (2012) Positive and negative allosteric modulators promote biased signaling at the calcium-sensing receptor. *Endocrinology* **153**(3): 1232-1241.

Diepenhorst NA, Leach K, Keller AN, Rueda P, Cook AE, Pierce TL, Nowell C, Pastoureau P, Sabatini M, Summers RJ, Charman WN, Sexton PM, Christopoulos A and Langmead CJ (2018) Divergent effects of strontium and calcium-sensing receptor positive allosteric modulators (calcimimetics) on human osteoclast activity. *Br J Pharmacol* **175**(21): 4095-4108.

Ehlert FJ (1988) Estimation of the affinities of allosteric ligands using radioligand binding and pharmacological null methods. *Mol Pharmacol* **33**(2): 187-194.

Geng Y, Mosyak L, Kurinov I, Zuo H, Sturchler E, Cheng TC, Subramanyam P, Brown AP, Brennan SC, Mun HC, Bush M, Chen Y, Nguyen TX, Cao B, Chang DD, Quick M, Conigrave AD, Colecraft HM, McDonald P and Fan QR (2016) Structural mechanism of ligand activation in human calcium-sensing receptor. *Elife* **5**: e13662.

Giraldo J (2015) Operational models of allosteric modulation: caution is needed. *Trends in pharmacological sciences* **36**(1): 1-2.

Huang Y, Zhou Y, Castiblanco A, Yang W, Brown EM and Yang JJ (2009) Multiple Ca(2+)-binding sites in the extracellular domain of the Ca(2+)-sensing receptor corresponding to cooperative Ca(2+) response. *Biochemistry* **48**(2): 388-398.

Keller AN, Kufareva I, Josephs TM, Diao J, Mai VT, Conigrave AD, Christopoulos A, Gregory KJ and Leach K (2018) Identification of Global and Ligand-Specific Calcium Sensing Receptor Activation Mechanisms. *Mol Pharmacol* **93**(6): 619-630.

Kenakin TP (2012) Biased signalling and allosteric machines: new vistas and challenges for drug discovery. *Br J Pharmacol* **165**(6): 1659-1669.

Leach K, Conigrave AD, Sexton PM and Christopoulos A (2015) Towards tissue-specific pharmacology: insights from the calcium-sensing receptor as a paradigm for GPCR (patho)physiological bias. *Trends in pharmacological sciences* **36**(4): 215-225.

Leach K, Davey AE, Felder CC, Sexton PM and Christopoulos A (2011) The role of transmembrane domain 3 in the actions of orthosteric, allosteric, and atypical agonists of the M4 muscarinic acetylcholine receptor. *Mol Pharmacol* **79**(5): 855-865.

Leach K, Gregory KJ, Kufareva I, Khajehali E, Cook AE, Abagyan R, Conigrave AD, Sexton PM and Christopoulos A (2016) Towards a structural understanding of allosteric drugs at the human calcium sensing receptor. *Cell Research* **26**: 574-592.

Leach K, Loiacono RE, Felder CC, McKinzie DL, Mogg A, Shaw DB, Sexton PM and Christopoulos A (2010) Molecular mechanisms of action and in vivo validation of an M4 muscarinic acetylcholine receptor allosteric modulator with potential antipsychotic properties. *Neuropsychopharmacology* **35**(4): 855-869.

Leach K, Sexton PM and Christopoulos A (2007) Allosteric GPCR modulators: taking advantage of permissive receptor pharmacology. *Trends in pharmacological sciences* **28**(8): 382-389.

May LT, Bridge LJ, Stoddart LA, Briddon SJ and Hill SJ (2011) Allosteric interactions across native adenosine-A3 receptor homodimers: quantification using single-cell ligand-binding kinetics. *FASEB J* **25**(10): 3465-3476.

Moreno Delgado D, Moller TC, Ster J, Giraldo J, Maurel D, Rovira X, Scholler P, Zwier JM, Perroy J, Durroux T, Trinquet E, Prezeau L, Rondard P and Pin JP (2017) Pharmacological evidence for a metabotropic glutamate receptor heterodimer in neuronal cells. *Elife* **6**.

Mutel V, Ellis GJ, Adam G, Chaboz S, Nilly A, Messer J, Bleuel Z, Metzler V, Malherbe P, Schlaeger EJ, Roughley BS, Faull RL and Richards JG (2000) Characterization of [(3)H]Quisqualate binding to recombinant rat metabotropic glutamate 1a and 5a receptors and to rat and human brain sections. *J Neurochem* **75**(6): 2590-2601.

Sato S, Huang XP, Kroeze WK and Roth BL (2016) Discovery and Characterization of Novel GPR39 Agonists Allosterically Modulated by Zinc. *Mol Pharmacol* **90**(6): 726-737.

Sengmany K and Gregory KJ (2016) Metabotropic glutamate receptor subtype 5: molecular pharmacology, allosteric modulation and stimulus bias. *Br J Pharmacol* **173**(20): 3001-3017.

Sengmany K, Hellyer SD, Albold S, Wang T, Conn PJ, May LT, Christopoulos A, Leach K and Gregory KJ (2019) Kinetic and system bias as drivers of metabotropic glutamate receptor 5 allosteric modulator pharmacology. *Neuropharmacology* **149**: 83-96.

Sengmany K, Singh J, Stewart GD, Conn PJ, Christopoulos A and Gregory KJ (2017) Biased allosteric agonism and modulation of metabotropic glutamate receptor 5: Implications for optimizing preclinical neuroscience drug discovery. *Neuropharmacology* **115**: 60-72.

Sinkins WG and Wells JW (1993) G protein-linked receptors labeled by [3H]histamine in guinea pig cerebral cortex. II. Mechanistic basis for multiple states of affinity [corrected]. *Mol Pharmacol* **43**(4): 583-594.

Stockton JM, Birdsall NJ, Burgen AS and Hulme EC (1983) Modification of the binding properties of muscarinic receptors by gallamine. *Mol Pharmacol* **23**(3): 551-557.

Storjohann L, Holst B and Schwartz TW (2008) Molecular mechanism of Zn2+ agonism in the extracellular domain of GPR39. *FEBS Lett* **582**(17): 2583-2588.

Vivo M, Lin H and Strange PG (2006) Investigation of cooperativity in the binding of ligands to the D(2) dopamine receptor. *Mol Pharmacol* **69**(1): 226-235.

Zhang C, Zhuo Y, Moniz HA, Wang S, Moremen KW, Prestegard JH, Brown EM and Yang JJ (2014) Direct determination of multiple ligand interactions with the extracellular domain of the calcium-sensing receptor. *J Biol Chem* **289**(48): 33529-33542.

Footnotes

Financial support

This work was supported by the National Health & Medical Research Council of Australia [Project Grants APP1085143 (KL), APP1138891 (KL, KJG), APP1084775 (KJG) and APP1127322 (KJG), Program Grant APP1055134 (AC) and Senior Principal Research Fellowship APP1102950 (AC)]; by the Australian Research Council (Discovery Grant DP170104228 (KL and KJG), and Future Fellowships FT160100075 (KL) and FT170100392 (KJG)]; and by the Ministerio de Ciencia, Innovación y Universidades of Spain [Project Grant SAF2017-87199-R (JG)].

Reprint requests to

Katie Leach

Drug Discovery Biology, Monash Institute of Pharmaceutical Sciences, Monash University, 399 Royal Parade, Parkville, 3052, Australia

katie.leach@monash.edu

Tables

Table 1. Simulation of agonist concentration-response relationships upon changes in binding or transducer slopes and τ_A. Data were simulated using the cooperative agonist operational model (Eq 2) and a Hill equation (Eq 9) was fitted to simulated data to determine agonist potency (pEC_{50}), maximum effect (E_{max}) and Hill slope (*nH*).

	Eq 2											
	***nB* 0.5**			***nB* 1**			***nB* 2**			***nB* 3**		
τ_A 1	**pEC_{50}**	**E_{max}**	***nH***	**pEC_{50}**	**E_{max}**	***nH***	**pEC_{50}**	**E_{max}**	***nH***	**pEC_{50}**	**E_{max}**	***nH***
***nT* 0.5**	4.8	51	0.3	3.9	50	0.7	3.4	50	1.3	3.3	50	2.0
***nT* 1**	3.5	51	0.5	3.2	51	1.0	3.1	51	2.0	3.0	51	3.0
***nT* 2**	2.6	51	0.6	2.8	51	1.3	2.8	51	2.4	2.9	51	3.5
***nT* 3**	2.2	52	0.7	2.6	52	1.4	2.7	52	2.9	2.8	52	4.1
τ_A 3	**pEC_{50}**	**E_{max}**	***nH***	**pEC_{50}**	**E_{max}**	***nH***	**pEC_{50}**	**E_{max}**	***nH***	**pEC_{50}**	**E_{max}**	***nH***
***nT* 0.5**	5.2	66	0.3	4.1	65	0.6	3.5	64	1.3	3.3	64	1.9
***nT* 1**	4.2	76	0.5	3.5	76	1.0	3.2	76	2.0	3.1	76	3.0
***nT* 2**	3.7	90	0.8	3.3	90	1.5	3.1	91	3.3	3.1	91	4.9

***nT* 3**	3.6	96	1.1	3.3	97	2.1	3.1	97	4.7	3.0	97	6.0

Table 2: Simulation of agonist concentration-response relationships upon changes in binding or transducer slopes and τ_A. Data were simulated using the Black and Leff model (Eq 1) or the cooperative agonist operational model (Eq 2) and a Hill equation (Eq 9) was fitted to simulated data to determine agonist potency (pEC_{50}), maximum effect (E_{max}) and Hill slope (*nH*).

	Eq 1; *nT* 1			**Eq 1; *nT* 3**			**Eq 2; *nT* 1, *nB* 1**			**Eq 2; *nT* 3, *nB* 3**			**Eq 2; *nT* 3, *nB* 3**		
τ_A	**pEC_{50}**	**E_{max}**	***nH***	**pEC_{50}**	**E_{max}**	***nH***	**pEC_{50}**	**E_{max}**	***nH***	**pEC_{50}**	**E_{max}**	***nH***	**pEC_{50}**	**E_{max}**	***nH***
100	4.9	99	1.0	4.9	100	3.0	4.9	99	1.0	3.6	99	3.0	3.6	100	8.9
10	4.0	91	1.0	3.9	100	2.7	4.0	91	1.0	3.3	91	3.0	3.2	100	7.6
1	3.2	51	1.0	2.6	50	1.5	3.2	51	1.0	3.0	51	3.0	2.8	51	4.5
0.3	3.0	24	1.0	2.4	3.0	1.4	3.0	24	1.0	3.0	24	3.0	2.7	3.0	3.9
0.1	3.0	9.0	1.0	2.3	0.1	1.4	3.0	9.0	1.0	3.0	9.0	3.0	2.7	0.1	3.8

Table 3: Quantification of Ca^{2+}_o affinity and efficacy for CaSR-Ca^{2+}_i mobilization using the operational model of agonism. Ca^{2+}_o concentration-response curves were generated at the WT receptor following overnight incubation of cells with or without 100 ng/mL tetracycline (tet) to induce receptor expression. For N-terminally truncated CaSRs, Ca^{2+}_o and Gd^{3+}_o concentration-response curves were generated upon induction of expression with 100 ng/mL tetracycline, where Ca^{2+}_o is a partial agonist and Gd^{3+}_o is a full agonist. The Black and Leff model (Eq 1) or the cooperative agonist operational model (Eq 2) was fitted to data to determine agonist affinity (pK_A), efficacy ($Log\tau_A$) or transducer or binding slope (*n*).

	WT		**N-terminally truncated CaSR**	
	Eq 1	**Eq 2**	**Eq 1**	**Eq 2**
pK_A (K_A; mM)	3.7 ±0.3 (0.2)	3.0 ±0.1 (1.0)	2.3 ±0.2 (5.0)	2.3 ±0.2 (5.0)
Logτ_A (τ_A)	100 ng/mL tet: 0.2 ±0.1 (1.6) 0 tet: -0.01 ±0.01 (1.0)	100 ng/mL tet: 1.2 ±0.2 (16) 0 tet: -0.1 ±0.1 (0.8)	0.2 ±0.1 (1.6)	0.2 ±0.1 (1.6)
n	6.0 ±3.0^	2.0 ±0.3^	1.0^^	1.0^^

^ An F test determined that data was fitted best when the binding or transducer slopes were different to unity (F data to test the hypothesis that n differed from 1: Eq 1 $p < 0.0001$, F ((Dfn, Dfd) 48.57 (1, 74); Eq 2 $p < 0.0001$, F (Dfn, Dfd) 45.78 (1, 74))

^^ An F test determined that data was fitted best when the binding or transducer slopes were not different to unity (F data to test the hypothesis that n differed from 1: Eq 1 p < 0.2282, F ((Dfn, Dfd) 1.470 (1, 101); Eq 2 p < 0.5332, F (Dfn, Dfd) 0.3970 (1, 101))

Table 4: Comparison of parameters describing CaSR allosteric interactions analyzed with different allosteric models. CaSR allosteric interactions with Ca^{2+}_o in intracellular Ca^{2+}_i mobilization assays were analyzed with the original operational model of agonism and allosterism (Eq 5 or 6) versus the operational model of allosterism with cooperative agonist binding (Eq 7 or 8) to determine Ca^{2+}_o potency (pEC_{50}), efficacy ($Log\tau_A$), or affinity (pK_A), modulator affinity (pK_B), cooperativity ($Log\alpha\beta$), transducer or binding slopes (n) and maximum system response (E_m).

	Ca^{2+}_o vs cinacalcet		**Ca^{2+}_o vs NPS2143**	
	Eq 5	**Eq 7**	**Eq 6**	**Eq 8**
pEC_{50}	3.3 ±0.01	3.3 ±0.01	n.d.	n.d.
pK_A (K_A, mM)	n.d.	n.d.	3.6 ±0.2 (0.3)	2.9 ±0.1 (1.3)
pK_B (K_B, μM)	6.3 ±0.04 (0.5)	5.8 ±0.1 (1.6)	6.6 ±0.04 (0.3)	7.3 ±0.1 (0.05)
$Log\tau_A$ (τ_A)	n.d.	n.d.	0.2 ±0.1 (1.6)	1.8 ±0.1 (63)
$Log\tau_B$ (τ_B)	n.a. (0)	n.a. (0)	n.a. (0)	n.a. (0)
$Log\alpha\beta$ ($\alpha\beta$)	0.5 ±0.01 (3.2)	1.4 ±0.1 (25)	-0.2 ±0.1 (0.6)	-1.7 ±0.1 (0.02)
n	2.8 ±0.1^	2.8 ±0.1^	12 ±4.0^	3.5 ±0.2^
E_m (% ionomycin)	79 ±1.0	80 ±1.0	78 ±1.0	80 ±2

^ An F test determined that data was fitted best when the transducer or binding slopes were different to unity (F data to test the hypothesis that n differed from 1: Eq 5 cinacalcet $p < 0.0001$, F ((Dfn, Dfd) 1249 (1, 2429); Eq 5 NPS2143 $p < 0.0001$, F ((Dfn, Dfd) 1022 (1, 908); Eq 7 cinacalcet $p < 0.0001$, F ((Dfn, Dfd) 1241 (1, 2429); Eq 7 NPS2143 $p < 0.0001$, F (Dfn, Dfd) 504.5 (1, 907))

n.d. = not determined

n.a. = no agonist activity, Logτ_B fixed to -100 (τ_B 0)

Table 5: Comparison of parameters describing $mGlu_5$ allosteric interactions analyzed with different allosteric models. $mGlu_5$ allosteric interactions with glutamate in intracellular $Ca^{2+}{}_i$ mobilization assays were analyzed with the original operational model of agonism and allosterism (Eq 3) or the operational model of allosterism with cooperative agonist binding (Eq 4) to determine modulator affinity (pK_B), glutamate or modulator efficacy ($Log\tau_A$ or $Log\tau_B$, respectively), cooperativity ($Log\alpha\beta$), transducer or binding slopes (n) and maximum system response (E_m).

	Glutamate vs MPEP[a]		**Glutamate vs M-5MPEP[a]**		**Glutamate vs VU29[b]**		**Glutamate vs DPFE[b]**	
	Eq 3	**Eq 4**	**Eq 3**	**Eq 4**	**Eq 3**	**Eq 4**	**Eq 3**	**Eq 4**
pK_A (K_A, μM)	6.2 (0.6)^	6.2 (0.6)^	6.2 (0.6)^	6.2 (0.6)^	6.2 (0.6)^	6.2 (0.6)^	6.2 (0.6)^	6.2 (0.6)^
pK_B (K_B, μM)	7.9 ±0.1 (0.01)	8.4 ±0.1 (0.004)	6.8 ±0.2 (0.2)	6.8 ±0.2 (0.2)	6.7 ±0.2 (0.2)	6.7 ±0.2 (0.2)	6.0 ±0.3 (1.0)	5.6 ±0.1 (2.5)
$Log\tau_A$ (τ_A)	0.7 ±0.1 (5.0)	1.0 ±0.2 (10)	0.6 ±0.1 (3.9)	0.6 ±0.2 (4.0)	0.7 ±0.03 (5.0)	0.7 ±0.1 (5.0)	0.6 ±0.1 (4.0)	0.8 ±0.1 (6.3)
$Log\tau_B$ (τ_B)	n.a. (0)	n.a. (0)	n.a. (0)	n.a. (0)	n.a. (0)	n.a. (0)	-0.2 ±0.1 (0.6)	-0.4 ±0.1 (0.4)
$Log\alpha\beta$ ($\alpha\beta$)	-100 (~0)^^	-100 (~0)^^	-0.5 ±0.1	-0.8 ±0.2	0.3 ±0.03	0.3 ±0.04	0.6 ±0.1	1.1 ±0.1 (13)

			(0.3)	(0.2)	(2.0)	(0.2)	(4.0)	
n	1.7 ±0.2^^^	1.5 ±0.2^^^	2.0 ±0.2^^^	1.6 ±0.2^^^	1.3 ±0.1^^^	1.2 ±0.1^^^	2.5 ±0.7^^^	1.3 ±0.1^^^
E_m (% glutamate)	106 ±6.0	111 ±6.0	107 ±6.0	123 ±1.0	108 ±3.0	112 ±3.0	107 ±2.0	105 ±2.0

^ pK_A was fixed to that determined in radioligand binding assays (Mutel et al., 2000)

^^ Log$\alpha\beta$ was fixed to -100 due to complete inhibition of glutamate-mediated stimulation of Ca^{2+}_i mobilization, reflecting high negative cooperativity

^^^ An F test determined that data was fitted best when the transducer or binding slopes were different to unity (F data to test the hypothesis that n differed from 1: Eq 3 MPEP p = 0.0003, F ((Dfn, Dfd) 13.46 (1, 149); Eq 3 M-5MPEP p = 0.0007, F ((Dfn, Dfd) 11.96 (1, 126); Eq 3 VU29 p = 0.0015, F ((Dfn, Dfd) 10.45 (1, 144); Eq 3 DPFE p = 0.0062, F (Dfn, Dfd) 7.587 (1, 294); Eq 4 MPEP p = 0.0002, F ((Dfn, Dfd) 14.33 (1, 149); Eq 4 M-5MPEP p < 0.0001, F ((Dfn, Dfd) 22.26 (1, 126); Eq 4 VU29 p = 0.0003, F ((Dfn, Dfd) 13.97 (1, 144); Eq 4 DPFE p < 0.0001, F (Dfn, Dfd) 24.13 (1, 294))

n.a. = no agonist activity, Logτ_B fixed to -100 (τ_B 0)

[a] Values derived by fitting previously reported experimental data (Sengmany et al., 2019)

[b] Values derived by fitting previously reported experimental data (Sengmany et al., 2017)

Molecular Pharmacology Fast Forward. Published on November 8, 2019 as DOI: 10.1124/mol.119.118091
This article has not been copyedited and formatted. The final version may differ from this version.

Table 6: Comparison of parameters describing M_4 mAChR allosteric interactions analyzed with different allosteric models. M_4 mAChR LY2033298 interactions with ACh in [^{35}S]GTPγS binding assays were analyzed with the original operational model of agonism and allosterism (Eq 3) or the operational model of allosterism with cooperative agonist binding (Eq 4) to determine agonist or modulator affinity (pK_A or pK_B, respectively), agonist or modulator efficacy (Logτ_A or Logτ_B, respectively), cooperativity (Log$\alpha\beta$), transducer or binding slopes (*n*) and maximum system response (E_m). Values obtained from fitting Eq 3 and Eq 4 to the data were identical and are therefore only presented in a single column.

	ACh vs LY2033298[a]
	Eq 3 and Eq 4
pK_A (K_A, μM)	6.0 (1.0)^
pK_B (K_B, μM)	5.9 ±0.3 (1.3)
Logτ_A (τ_A)	0.9 ±0.1 (7.9)
Logτ_B (τ_B)	0.5 ±0.2 (3.2)
Log$\alpha\beta$ ($\alpha\beta$)	0.7 ±0.3 (5.0)
n	1.0^^
E_m (% ACh max)	112 ±5.0

[a] Data analyzed is from (Leach et al., 2010)

^ pK_A was fixed to that determined in radioligand binding assays (Leach et al., 2010)

^^ An F test determined that data was fitted best when the transducer or binding slopes were not different to unity (F data to test the hypothesis that n differed from 1: Eq 3 p = 0.5766, F ((Dfn, Dfd) 0.3129 (1, 172); Eq 4 p = 0.4541, F ((Dfn, Dfd) 0.5629 (1, 172))

Molecular Pharmacology Fast Forward. Published on November 8, 2019 as DOI: 10.1124/mol.119.118091
This article has not been copyedited and formatted. The final version may differ from this version.

Figure Legends

Figure 1. *nT* and *nB* differentially contribute to agonist concentration-response relationships. Simulations demonstrating the influence of *nT* or *nB* on concentration-response relationships for agonists with different efficacies (τ_A). Data were simulated using the cooperative agonist operational model (Eq 2), where the affinity of the agonist (K_A) is 1.2 mM and *nT* or *nB* are between 1 and 3. Curves through the data are the fits to a 4 parameter Hill equation (Eq 9), where parameters describing the fits are shown in Table 1.

Figure 2. Cooperative agonist binding influences agonist concentration-response relationships. Simulations demonstrating the influence of agonist efficacy (τ_A) on agonist concentration-response relationships when the slope is governed by the transducer slope (*nT*, Black and Leff operational model of agonism) or by the agonist binding slope (*nB*, cooperative agonist operational model). Data were simulated using the Black and Leff model (Eq 1) or the cooperative agonist operational model (Eq 2), where the affinity of the agonist (K_A) is 1.2 mM and *nT* or *nB* are between 1 and 3. Curves through the data are the fits to a Hill equation (Eq 9), where parameters describing the fits are shown in Table 2.

Figure 3. Ca^{2+}_o-CaSR concentration-response relationships fit well to the cooperative agonist operational model. (A) Ca^{2+}_o-mediated Ca^{2+}_i mobilization at the WT CaSR following overnight receptor induction with 100 ng/mL tetracycline (tet) or in the absence of tetracycline. Data are mean + SD from 4 independent experiments performed in duplicate. Curves through the data are the fits to the Black and Leff model (blue line) or the cooperative agonist operational model (red line), where parameters describing the fits are shown in Table 3. Although both models fit the data, the cooperative agonist operational model more accurately predicts the expected affinity of Ca^{2+}_o at the CaSR (Table 3). (B) Gd^{3+}_o and Ca^{2+}_o

Molecular Pharmacology Fast Forward. Published on November 8, 2019 as DOI: 10.1124/mol.119.118091
This article has not been copyedited and formatted. The final version may differ from this version.

concentration-response curves at the WT CaSR following overnight receptor induction with 100 ng/mL tetracycline. Data are mean + SD from 4 independent experiments performed in duplicate. Curves through the data are the fits to a 4 parameter Hill equation. (C) N terminally-truncated CaSR snake diagram. (D) Gd^{3+}_o and Ca^{2+}_o concentration-response curves at an N terminally-truncated CaSR following overnight receptor induction with 100 ng/mL tetracycline. Data are mean + SD from 5 independent experiments performed in duplicate. Curves through the data are the fits to the cooperative agonist operational model, where parameters describing the fits are shown in Table 3.

Figure 4. Allosteric modulation at the CaSR is fitted well by an operational model of allosterism with cooperative agonist binding. Allosteric modulation of Ca^{2+}_o-mediated Ca^{2+}_i mobilization at the CaSR by NPS2143 (NAM) or cinacalcet (PAM). Data were previously published (Leach et al., 2016) and are mean + SD from at least 11 independent experiments performed in duplicate. Curves through the data are the fits to the operational model of allosterism with cooperative agonist binding and contaminating agonist (Eq 7 for cinacalcet and Eq 8 for NPS2143), where parameters describing the fits are shown in Table 4.

Figure 5. Allosteric modulation at $mGlu_5$ is fitted well by an operational model of allosterism with cooperative agonist binding. Allosteric modulation of glutamate-mediated Ca^{2+}_i mobilization at $mGlu_5$ by MPEP (full NAM), M-5MPEP (partial NAM), VU-29 (PAM) and DPFE (ago-PAM). Data were previously published (Sengmany et al., 2019; Sengmany et al., 2017) and are mean + SD from at least 3 independent experiments performed in duplicate previously published. Curves through the data are the fits to the operational model of allosterism with cooperative agonist binding (Eq 4), where parameters describing the fits are shown in Table 5.

Molecular Pharmacology Fast Forward. Published on November 8, 2019 as DOI: 10.1124/mol.119.118091
This article has not been copyedited and formatted. The final version may differ from this version.

Figure 6. Allosteric modulation at the M_4 mAChR is fitted well by an operational model of allosterism with no cooperative agonist binding. Positive modulation of ACh-mediated [^{35}S]GTPγS binding by LY2033298 (ago-PAM) at the M_4 mAChR. Data were previously published (Leach et al., 2010) and are mean + SD from at least 3 independent experiments performed in duplicate. Curves through the data are the fits to the operational model of allosterism with cooperative agonist binding (Eq 4), where the Eq was fitted best when n=1 (i.e. no cooperative agonist binding). Parameters describing the fits are shown in Table 6.

Figure 7. Modulator affinity and cooperativity are influenced by assignment of the slope in the operational model of allosterism. Simulations demonstrating the influence of the agonist binding slope on estimated modulator affinity and cooperativity when interaction data are analyzed using the original operational model of allosterism. Interaction data between an orthosteric agonist and a NAM or PAM were simulated with the operational model of allosterism with cooperative agonist binding. Orthosteric agonist affinity (1 μM), τ_A (10), and modulator affinity (10 nM) were held constant, and different magnitudes of positive or negative cooperativity were examined alongside changes in the magnitude of cooperative agonist binding. The simulated data were analyzed with the original operational model of allosterism, and LogK_B (A) or Logαβ (B) estimates were plotted against the agonist binding slope.

Molecular Pharmacology Fast Forward. Published on November 8, 2019 as DOI: 10.1124/mol.119.118091
This article has not been copyedited and formatted. The final version may differ from this version.

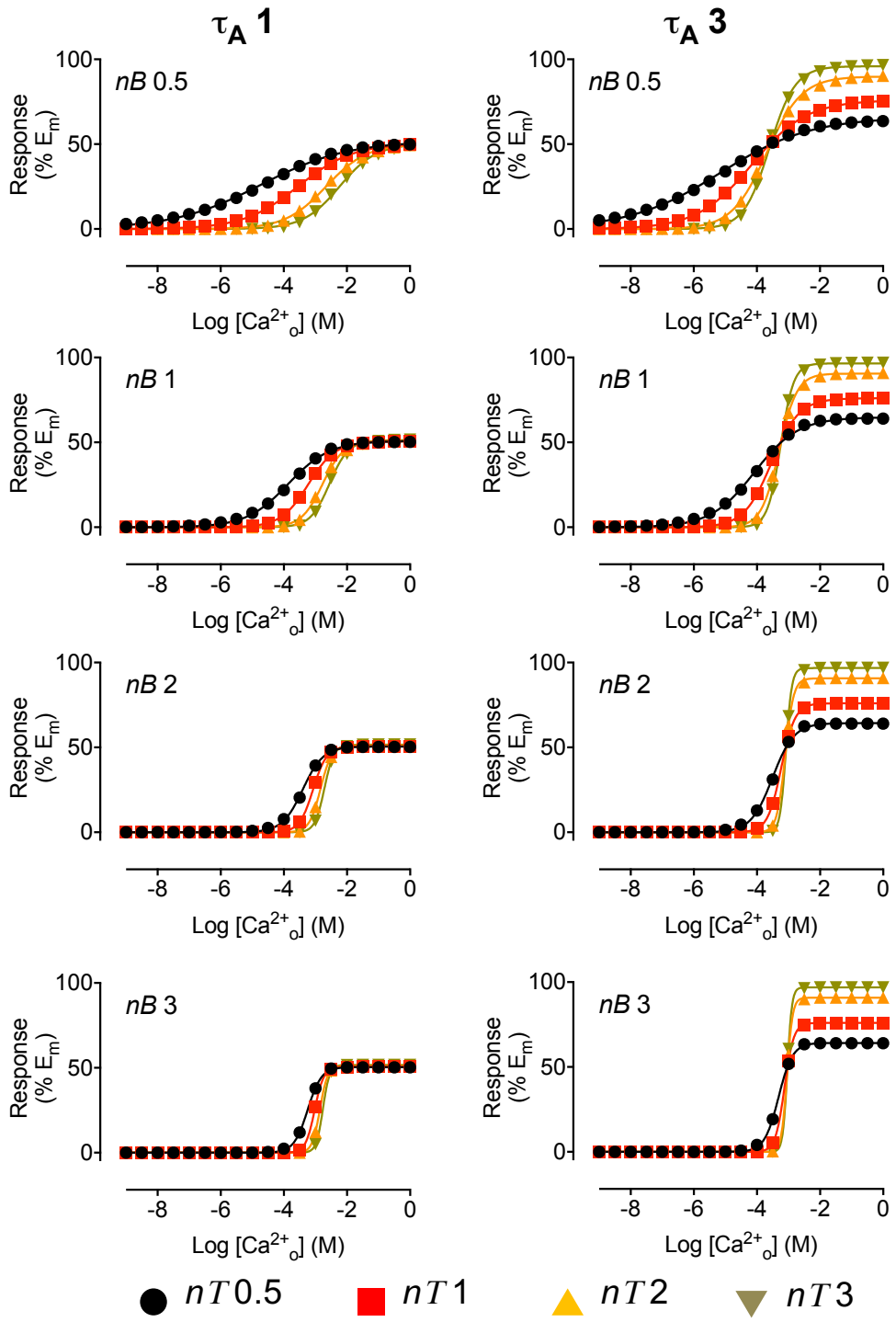

Molecular Pharmacology Fast Forward. Published on November 8, 2019 as DOI: 10.1124/mol.119.118091
This article has not been copyedited and formatted. The final version may differ from this version.

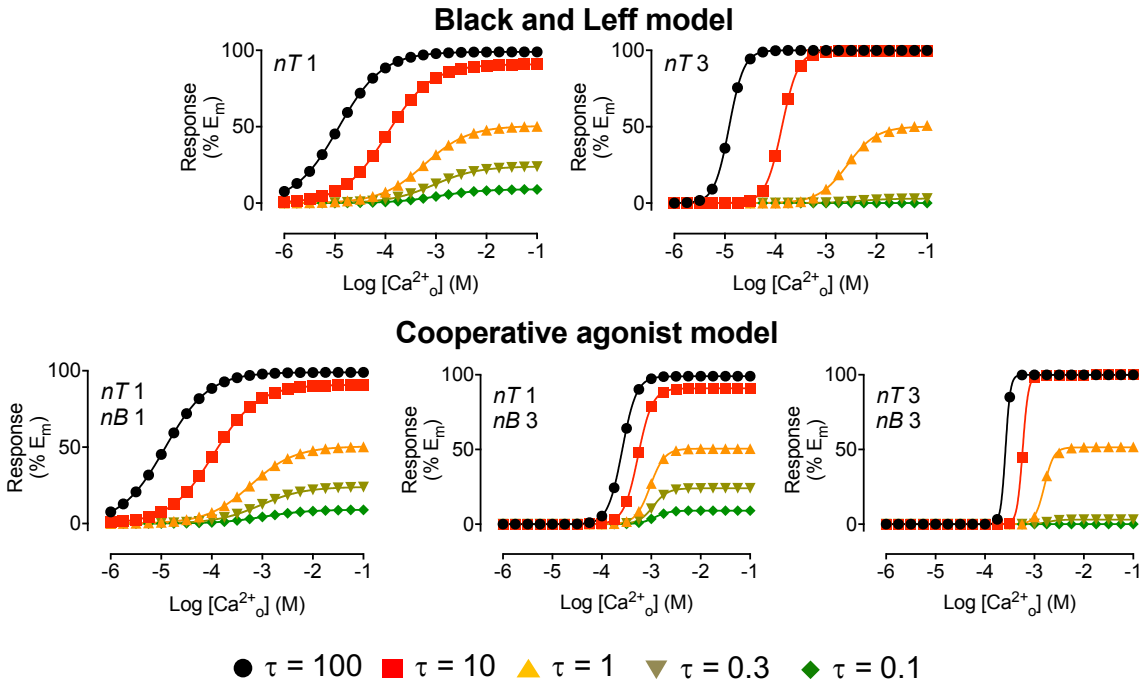

Molecular Pharmacology Fast Forward. Published on November 8, 2019 as DOI: 10.1124/mol.119.118091
This article has not been copyedited and formatted. The final version may differ from this version.

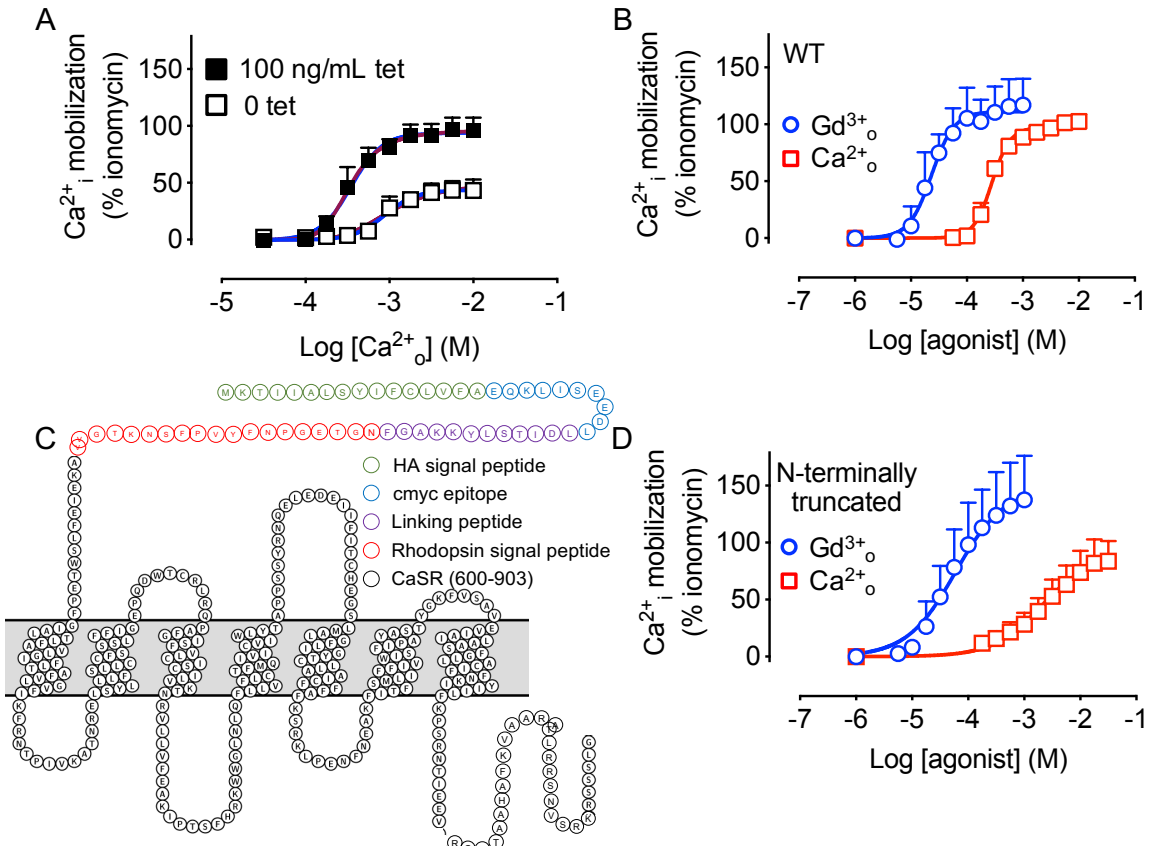

Molecular Pharmacology Fast Forward. Published on November 8, 2019 as DOI: 10.1124/mol.119.118091
This article has not been copyedited and formatted. The final version may differ from this version.

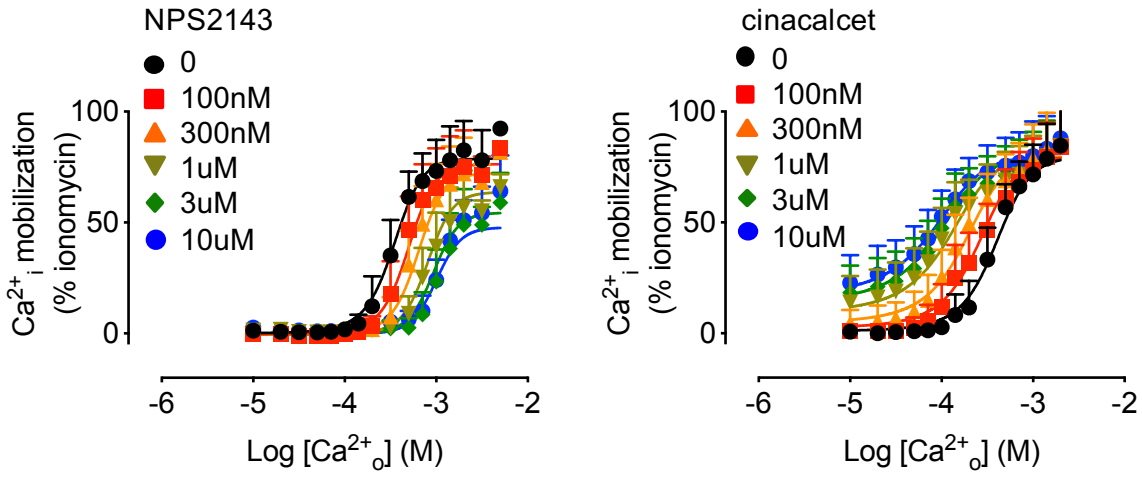

Molecular Pharmacology Fast Forward. Published on November 8, 2019 as DOI: 10.1124/mol.119.118091
This article has not been copyedited and formatted. The final version may differ from this version.

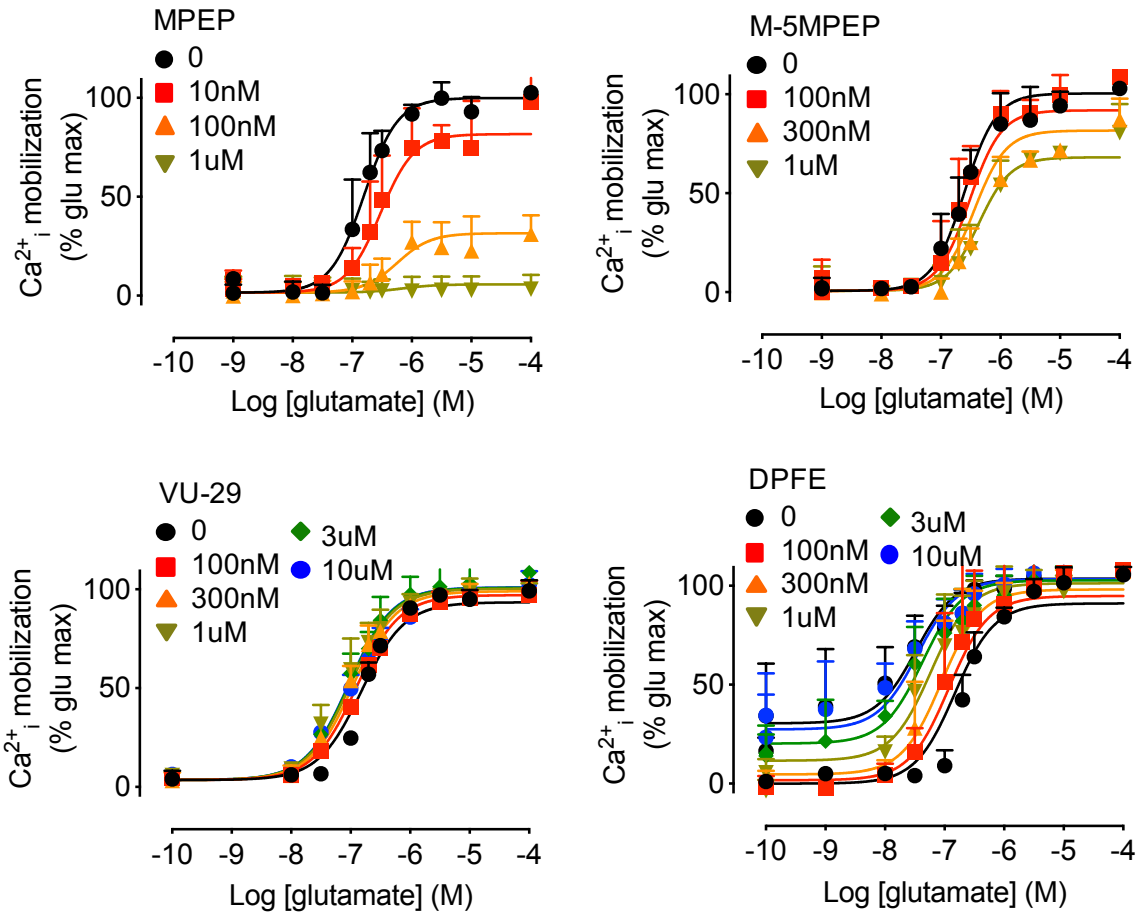

Molecular Pharmacology Fast Forward. Published on November 8, 2019 as DOI: 10.1124/mol.119.118091
This article has not been copyedited and formatted. The final version may differ from this version.

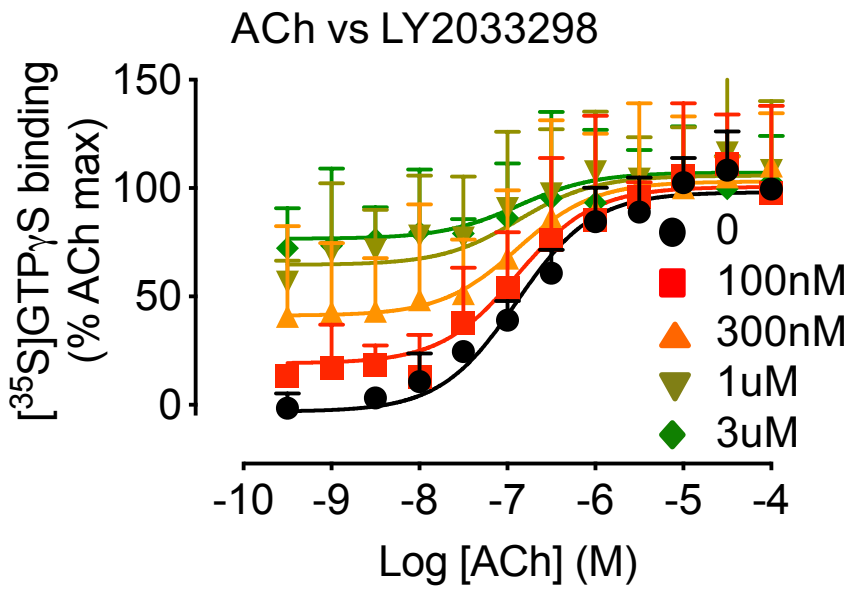

Molecular Pharmacology Fast Forward. Published on November 8, 2019 as DOI: 10.1124/mol.119.118091
This article has not been copyedited and formatted. The final version may differ from this version.